ISME2016-21576

Experimental investigations on energy absorption behavior of thin-walled end-capped steel cones effected by stepped initiators

M.Shariati[1], E.Sanati[2], S.Nazarian[3]
[1]Professor, Ferdowsi University of Mashhad, Faculty of Engineering, Department of mechanical engineering;
Tel: 05138805159, mshariati44@um.ac.ir and mshariati44@gmail.com
[2]BSc student, Ferdowsi University of Mashhad, Faculty of Engineering, Department of mechanical engineering;
elahe_sanaty@yahoo.com
[3] BSc student, Ferdowsi University of Mashhad, Faculty of Engineering, Department of mechanical engineering;
nazari_sa2008@yahoo.com

Abstract

Generally, when a cone is directly put under axial loading as an energy absorber, a rather big peak load is observed in the linear behavior of the load-displacement curve that is considered harmful. To decrease this initial peak load, one can use some kind of initiator.

This paper deals with experimental axial quasi static loading tests on the effect of stepped initiators in thin walled steel end capped conical tubes.

The initiator used in this paper is in fact a solid bar with an adjustable length that applies axial loading vertically on the closed surface of the cone. In order to decrease the stiffness of initiators two to four holes with specific layouts are extruded through the end-capped part of cones. First, the initiator functions to decrease the initial stiffness. Then, a solid plate applies loading on the cone to develop the desired deformation of the cone served as energy absorption.

In addition, some parameters such as the energy absorption E, specific energy absorption, SEA, and crush force efficiency, CFE have been considered to illuminate the efficiency of the initiators and constraint forces in this crash absorbers.

Keywords: energy absorption, quasi-static loading, end-capped cones, specific energy absorption, crush force efficiency

1. Introduction

Design optimization represents a key area of rapid development in automotive and aerospace industries over the past decades. On one hand, energy crisis and environmental concerns place higher requirements in light weight and usage of materials and fuels. On the other hand, socioeconomics and healthcare demand raises stricter technical requirements in road safety. The former typically reduces weight and save space, while the other often needs to go an opposite way. Besides, industries are required to handle finance problems as well. For these reasons, crashworthiness design of vehicular structures and components draw considerable attention and major effort has been made to balance them by maximizing the energy absorption and minimizing impact forces with minimum weight and cost. In this regard, thin walled structures have been proven fairly effective and been widely studied and employed in vehicles.

One of the simple structural elements is the conical tube that traditionally was made in steel because of its low cost and excellent ductility.

The early studies on crashworthy characteristics of conical shells was carried by Postleth Waite and Mills [1], where Alexander's extensible collapse analysis for rigid-perfectly material cones was presented. Mamalis et al [2-4] reported some experimental results of axial crushing of aluminum and steel cylinders and frusta of 5° and 10° apical angles and produced an expression for the crushing load by fitting the experimental results corresponding to various modes(axisymmetric rings and diamond). Also, according to investigations of Sheriff N. Mohamed and Gupta N.K [5], thin walled conical tubes under crushing load achieve similar crushing modes as cylindrical tubes based on their length and cross-section dimensions. They collapse in axisymmetric mode (concertina or ring mode), non-axisymmetric mode (diamond mode) or mixed mode. Energy absorption normally takes place progressive buckling of the tubes' walls. Easwara Prasad and Gupta [6] performed some crush experiments on conical frusta samples with large-semi apical angles at various strain rates. Numerical and experimental studies were carried out by Gupta et al [7] to investigate the influence of the rolling and stationary plastic hinges in the post-buckling pattern of the quasi statically loaded conical tubes. They finally compared their experimental and numerical results. Gupta and Venkatesh [8] reported experimental studies to investigate the crush performance of conical frusta tubes subjected to quasi-static and dynamic axial crush loadings. A. Ghamarian and M.T Abadi [9, 10] investigated the conical end capped tubes. Their experiments showed that under the same crush condition, the initial peak load of the end-capped tubes is lower than the non-end-capped ones. Also, the deceleration pulse created by the end-capped tubes is lower. Hence, the end-capped tubes are convenient shock absorbers for structures which are sensitive to deceleration level. Petsios [11] conducted a comprehensive and dynamic testing program on frusta to study the buckling of it. A. Ghamarian and H. Zarei investigated the crash performance of the end-capped cylindrical and conical tubes under axial quasi-static loading experimentally and numerically. Other axial collapse models and energy absorption characteristics of conical shells have been reported in refs. [12- 15]

Since the use of stepped initiators has not become common for conical tubes, in this paper, the crash

performance of the end-capped conical steel tubes with specific initiators (two to four holes extruded on the end part of the conical tubes) and under different loading is studied experimentally.

2. Experimental test procedure

2.1 Setup and material properties

The end-capped conical tubes were fabricated from steel plates using a spinning process. The circular coupons were cut from steel plates of a thickness of 1.1 and 0.6 mm and stretched over the surface of a rotating die. The thickness of the end of the tubes is the same as the coupons' thickness, while there is some thickness gradient observed in the tubes' walls due to stretching of the coupons over the die surface. Also the specimens where nominated as follows: Cone Steel-D-50.5-d1-40mm-d2-42mm-d3-10mm-d4-20mm-m-10mm-2Holes-h52.5-t1.1mm, that includes the tubes' height h, diameters D and d_1 and d_2 which are the bottom and top diameters of the conical tubes, respectively, d_3 that is the diameter of the extruded holes on the top of the conical tubes as the initiators, d_4 which is the diameter of the rigid bar that applies load after initiator, the length of the bar m and wall thickness t. The numbers following D, d_1, d_2, d_3, d_4, m and h quantify these dimensions for the specimens. The wall thickness is measured at the close and open edges of the tubes' walls. Fig (1) shows the schematic of the end-capped cone and the initiator.

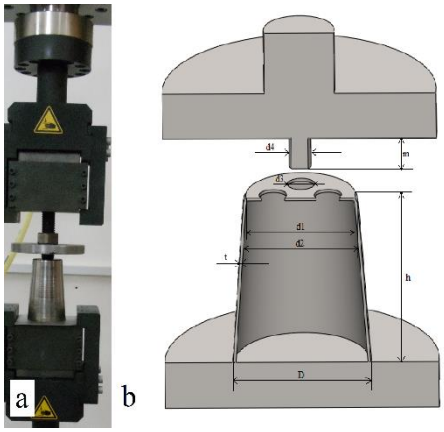

Fig 1: (a) Sample setup of one of the conical end capped tube, (b) Geometrical details of the specimen and the initiator

Here, the main objective is to study the effect of a special initiator as well as a special kind of loading on peak load, average load, energy absorption and specific energy absorption. Quasi-static loading tests were carried out by a Zwick/Roel Amsler HB100 machine in fatigue laboratory of Ferdowsi university of Mashhad.

2.2 Investigated parameters

Selected parameters in this investigation that are used for comparison and could be achieved from load-displacement curve are as follows:

1. Maximum crushing load – maximum crushing load, P_{max}, is the maximum force in load-displacement curve and often occurs at the initial stage of loading when the first folding happens. This parameter is important in optimum design of energy absorbers and attempt is to reduce its value.
2. Total absorbed energy – this parameter shows the total energy consumed during structure deformation and is equal to area under load–displacement curve which is obtained from the following equation:
   $$E_{absorbed} = \int P\, d\delta \quad (1)$$
   Where P and dδ are crushing load and crushing displacement, respectively.
3. Average crushing load – average load, P_m, is obtained by dividing the measured absorbed energy to the total crushing distance δ_t:
   $$P_m = \frac{1}{\delta_t}\int P\, d\delta \quad (2)$$
4. Crush force efficiency – this parameter, CFE, is used to compare efficiencies of energy absorbers and is defined as the ratio of average/maximum crushing loads:
   $$CFE = \frac{P_m}{P_{max}} \quad (3)$$
5. Specific absorbed energy – this parameter, SAE, is absorbed energy, $E_{absorbed}$, per unit mass of structure, M:
   $$SAE = \frac{E_{absorbed}}{M} \quad (4)$$

2.3 Experimental results

Fig (1) shows a picture of one of the conical tubes to illustrate the experimental setup. Initially, the tubes where placed symmetrically on the bottom die of the testing machine and the actuator was pressed downwards into the conical tube until the initiator bar was tangential to the surface of end-capped cone. After that, the testing machine was started to press the actuator towards the bottom die till the tube was completely deformed. The driving load-displacement curves, i.e. L-D curves, obtained from the tests will be discussed in the next section. It should be mentioned that the tests were divided into two categories. The first category investigates the effect of different lengths of initiator bar as the applier force, individually and the second one studies the effect of special numbers of holes as initiators while the length of the loading bar changes.

2.3.1 First category: various length of loading bars

Three different lengths of the loading bar were compared with a simple plate as loading. Fig (2-9) show these four cases during and after the tests with their L-D diagrams.

2.3.2 Second category: the effect of special numbers of holes as initiators

Three different numbers of holes (two, three and four) were compared with a simple conical tube. Fig (10-17) show these tubes in these four cases during and after the tests with their L-D curves.

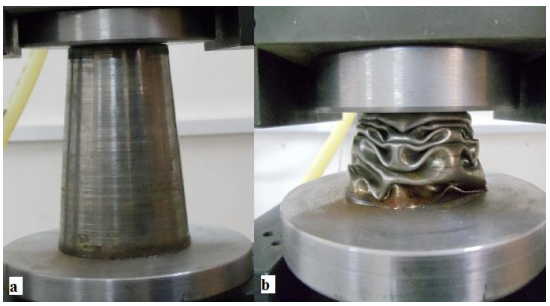

Fig 2: Steel Cone-D-67.1-d1-47.2-d2-51.2-h-100.5-t-0.6mm (a) before test, (b) after test

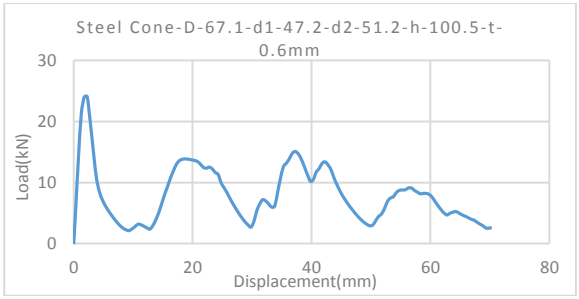

Fig 3: L-D curve of Steel Cone-D-67.1-d1-47.2-d2-51.2-h-100.5-t-0.6mm

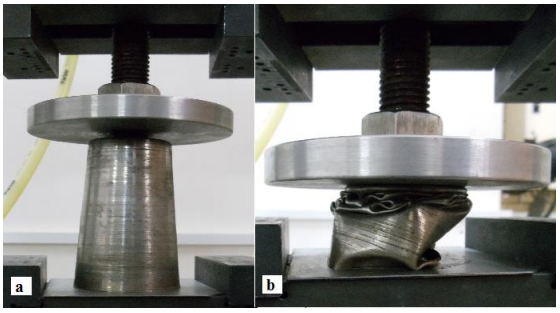

Fig 4: Steel Cone- D-67.1-d1-47.2-d2-51.2-d3-24-m-5mm-h-100.5-t-0.6mm (a) before test, (b) after test

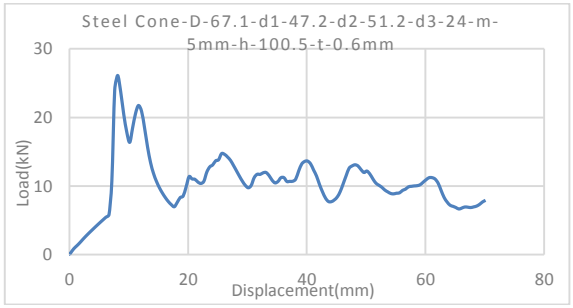

Fig 5: L-D curve of Steel Cone- D-67.1-d1-47.2-d2-51.2-d3-24-m-5mm-h-100.5-t-0.6mm

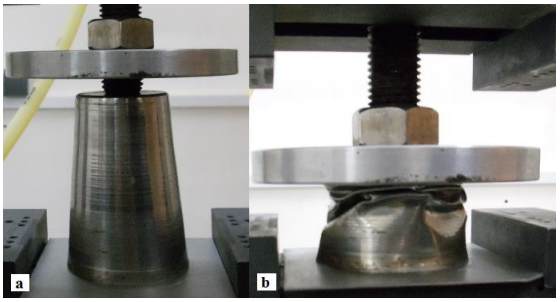

Fig 6: Steel Cone- D-67.1-d1-47.2-d2-51.2-d3-24-m-10mm-h-100.5-t-0.6mm (a) before test, (b) after test

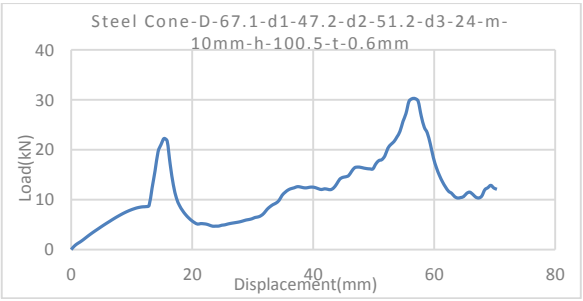

Fig 7: L-D curve of Steel Cone- D-67.1-d1-47.2-d2-51.2-d3-24-m-10mm-h-100.5-t-0.6mm

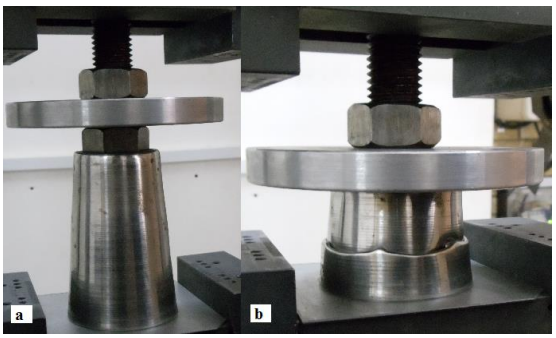

Fig 8: Steel Cone- D-67.1-d1-47.2-d2-51.2-d3-24-m-18.2mm-h-100.5-t-0.6mm (a) before test, (b) after test

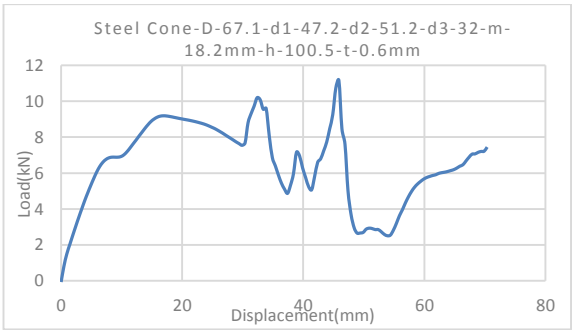

Fig 9: L-D curve of Steel Cone- D-67.1-d1-47.2-d2-51.2-d3-24-m-18.2mm-h-100.5-t-0.6mm

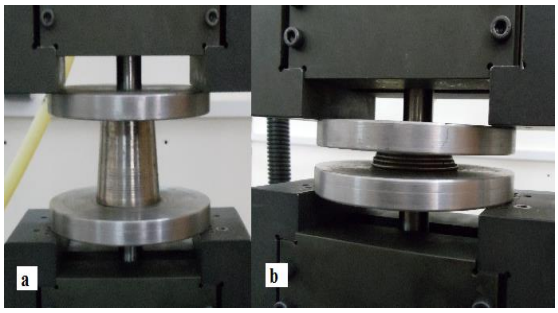

Fig 10: Cone Steel-D-50.5-d1-40mm-d2-42mm-h-52.5-t-1mm (a) before test, (b) after test

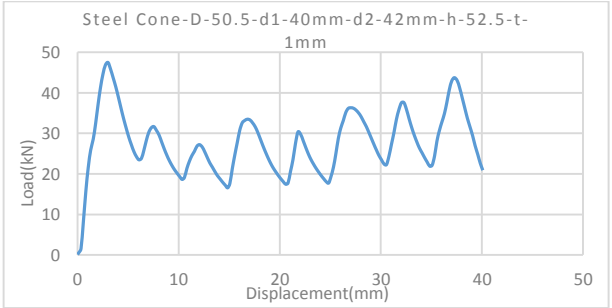

Fig 11: L-D curve of Cone Steel-D-50.5-d1-40mm-d2-42mm-h-52.5-t-1mm

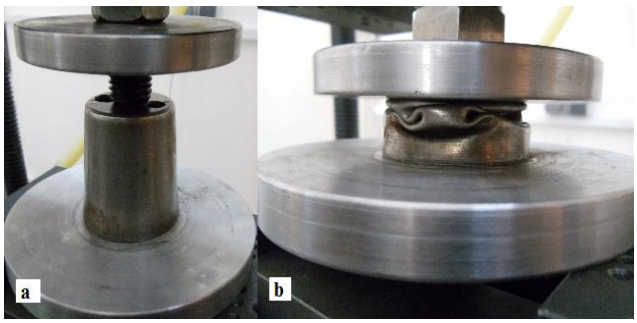

Fig 12: Cone Steel-D50.5-d1-40mm-d2-42mm-d3-10mm-d4-20mm-m-17.5mm-2Holes-h52.5-t1mm
(a) before test, (b) after test

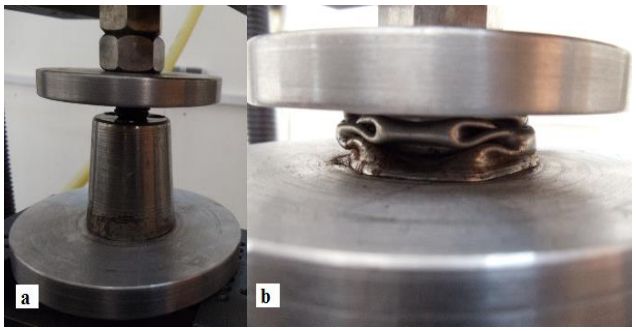

Fig 14: Cone Steel-D50.5-d1-40mm-d2-42mm-d3-10mm-d4-20mm-m-10mm-3Holes-h52.5-m10mm-t1mm
(a) before test, (b) after test

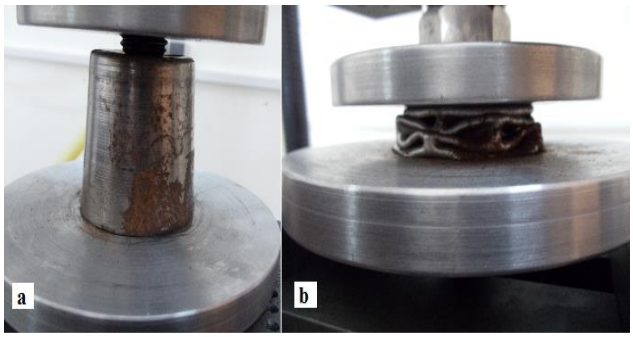

Fig 16: Cone Steel-D50.5-d1-40mm-d2-42mm-d3-10mm-d4-20mm-m-5mm-4Holes-h52.5-m5mm-t1mm
(a) before test, (b) after test

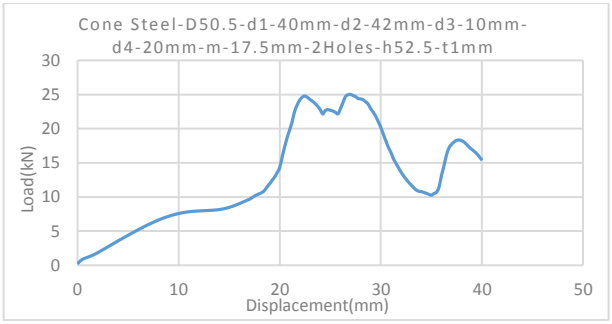

Fig 13: L-D curve of Cone Steel-D50.5-d1-40mm-d2-42mm-d3-10mm-d4-20mm-m-17.5mm-2Holes-h52.5-t1mm

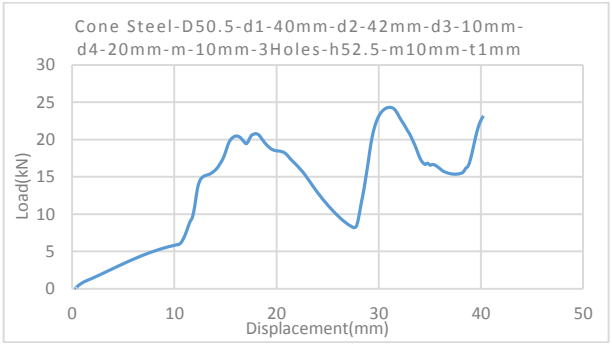

Fig 15: L-D curve of Cone Steel-D50.5-d1-40mm-d2-42mm-d3-10mm-d4-20mm-m-10mm-3Holes-h52.5-m10mm-t1mm

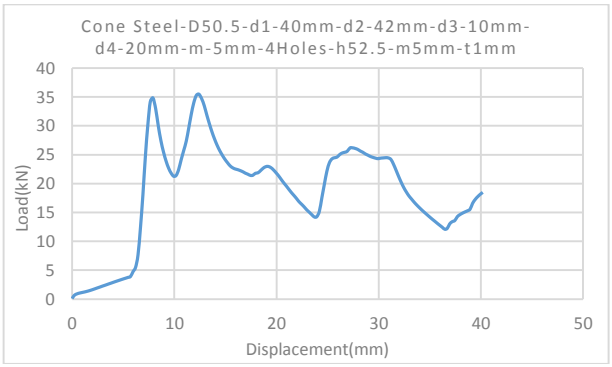

Fig 17: L-D curve of Cone Steel-D50.5-d1-40mm-d2-42mm-d3-10mm-d4-20mm-m-5mm-4Holes-h52.5-m5mm-t1

3. Discussion

For all of the specimens, the driving force continuously increases with oscillation and drops rapidly after the initial rising stage during the whole pressing process and no steady state force can be found. It was observed that the use of initiators and different actuators not only affect the shape of L-D curves, but also influence the characteristics of the tube's deformation.

There is a logical relation between load–displacement curve and deformation of tubes and this correlation is discussed here.

The L-D curves of the first category indicates that the use of loading bars decreases the first peak load, but somehow in other stages of the crushing process increases the maximum load except for the loading bar with the length of 18.2 mm that has the least maximum load and absorbed energy because of the increase in d_4. Generally, when the loading process transforms from elastic to plastic and the first folding is formed, load is reduced suddenly. But this stage was just observed for the two simple conical tubes with the rigid loading plate. For other cases, when the end part of the tube which is in contact with the loading bar enters the plastic stage, the walls are still having the elastic deformation. After the rigid plate meets the tube, the L-D curve tends to increase even more and then drop rapidly or constantly in different cases.

Each maximum point in load-displacement curve is equivalent to one new folding in tubes. The load decreases after initiation of each folding and when two edges of each folding meet each other, load increases up to next maximum point and this process repeats before complete deformation of the conical tubes. Then the specimen act as a relatively rigid body and load increases severely without considerable excess deformation.

The highest amount of $E_{absorbed}$, SAE, P_{max} and P_m belongs to the tube under loading of the bar with m=10mm, but it has the least crush force efficiency. (See table 1)

Table 1: Test results for conical end-capped tubes with various length of loading bar

Number	1	2	3	4
Specimen code	Cone Steel-D67.1-d1-47.2-d2-51.2-h100.5-t0.6mm	Cone Steel-D67.1-d1-47.2-d2-51.2-d4-24-m5mm-h100.5-t0.6mm	Cone Steel-D67.1-d1-47.2-d2-51.2-d4-24-m10mm-h100.5-t0.6mm	Cone Steel-D67.1-d1-47.2-d2-51.2-d4-32-m18.2mm-h100.5-t0.6mm
Crushing length(mm)	70.3078	70.1666	70.3945	70.3866
$E_{absorbed}$(J)	561.7804	738.2457	822.1200	459.1508
P_{max}(kN)	24.0452	26.1229	30.2625	11.1615
P_m(kN)	3.42	3.72	4.30	1.59
CFE (%)	14.22	14.24	14.21	14.25
SAE(J/kg)	5526.61	7361.84	7915.66	5178.78

Table 2: Test results for conical end-capped tubes with initiators

Number	1	2	3	4
Specimen code	Cone Steel-D50.5-d1-40mm-d2-42mm-h52.5-t1mm	Cone Steel-D50.5-d1-40mm-d2-42mm-d3-10mm-d4-20mm-m-17.5mm-2Holes-h52.5-t1mm	Cone Steel-D50.5-d1-40mm-d2-42mm-d3-10mm-d4-20mm-m-10mm-3Holes-h52.5-m-10mm-t1mm	Cone Steel-D50.5-d1-40mm-d2-42mm-d3-10mm-d4-20mm-m-5mm-4Holes-h52.5-m5mm-t1mm
Crushing length(mm)	40.0928	40.0042	39.9170	40.1701
$E_{absorbed}$(J)	1109.6	509.7032	528.0045	748.7705
P_{max}(kN)	47.4563	25.0456	24.3109	35.4723
P_m(kN)	11.837	6.261	6.090	8.831
CFE (%)	24.94	25	25.05	24.90
SAE(J/kg)	15950	9390	9620	11640

For the tubes with holes as initiators it was noticed that extrusion of holes decreases the absorbed energy, maximum force, mean force and specific absorbed energy. Therefore, after testing the conical tube with two holes, another method was proceeded. As it was determined before, the decrease in the length of loading bar increases the crush force efficiency. Thus, this length was reduced in the proceeding tests and as table 2 shows, there was an elevation in $E_{absorbed}$, P_{max}, P_m and CFE.

The comparison between the L-D curves of each categories are shown in Fig (18) and Fig (19).

It should be noted that all the conical tubes used in present experiments were compressed uniformly and no fracture, local buckling or wrinkling was observed in the tests.

4. Conclusions

- The more the length of the loading bar, the higher absorbed energy, maximum load, mean load, crush force efficiency and SAE.
- Comparison between the third and fourth row of table 1 proves that enlargement of loading bar's dimension (d_4), lessens all the invested parameters except for CFE.
- The use of extruded holes as part of the initiators in conical tubes reduces all the invested parameters. Hence, it is not recommended as an effective initiator.
- Comparison between the first rows of both tables demonstrates that doubling the height of the conical tube with negligible difference in other dimensions, almost halves the invested parameter.

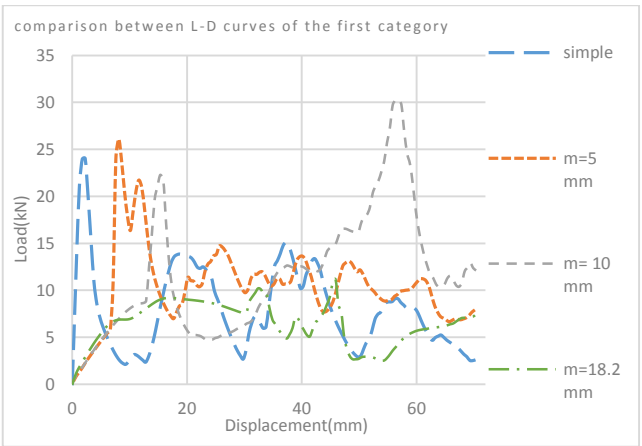

Fig 18: Comparison between L-D curves of the 1st category

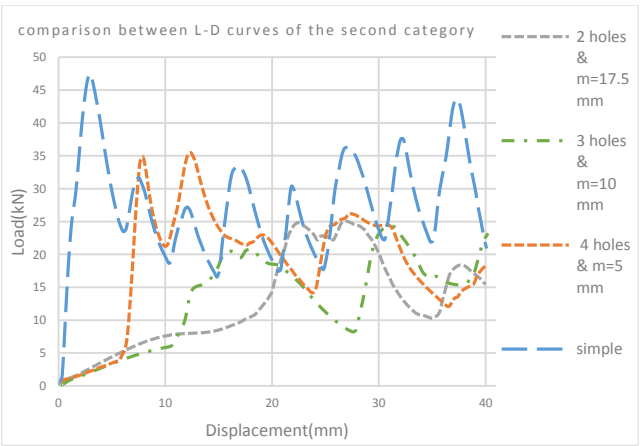

Fig 19: Comparison between L-D curves of the 2nd category

5. References

[1] Postleth Waite HE, Mills B, 1970. "Use of collapsible structural elements as impact isolators with special reference to automotive applications". J strain Anal, 5, pp.58-73.

[2] Mamalis AG, Johnson W, 1983. "The quasi static crumpling of thin walled circular cylinders and frusta under axial compression". Int J Mech Sci, 25(9), pp.713-32.

[3] Mamalis AG, Johnson W, Viegelahn GL, 1984. "The crumpling of thin walled tubes and frusta under axial compression at elevated strain rates: some experimental results". Int J Mech Sci, 26(11-12), pp.537-47.

[4] Mamalis AG, Manolakos DE, Saigal S, Viegelahn G, Johnson W, 1986. "Extensible plastic collapse of thin walled frusta as energy absorbers". Int J Mech Sci, 28(4), pp.219-29.

[5] Sheriff N. Mohamed, Gupta N.K, Velmurugan R, Shanmugapriyan N, 2008. "Optimization of thin conical frusta for impact energy absorption". Thin-walled. Struc. J, 46, pp.653-666.

[6] Easwara Prasad G.L and Gupta N.K, 2005. "An experimental study of deformation modes of domes and large-angled frusta at different rates of compression". Int. J. Impact. Eng, 32, pp.400-415.

[7] Gupta N.K, Sheriff N. Mohamed, Velmurugan R, 2006. "A study on buckling of thin conical frusta under axial loads". Thin-Walled Struc. J, 44, pp.986-996.

[8] Gupta N.K, Venkatesh R, 2007. "Experimental and numerical studies of impact axial compression of thin-walled conical shells". Int. J. Impact. Eng, 34, pp.708-720.

[9] Ghamarian A, Abadi M.T, 2011. "Axial crushing analysis of end-capped circular tubes". Thin-Walled Struc. J, 49, pp.743-752.

[10] Ghamarian A, Zarei H.R, Abadi M.T, 2011. "Experimental and numerical crash worthiness investigation of empty and foam-filled end-capped conical tubes". Thin-Walled Struc. J, 49, pp.1312-1319.

[11] Petsios M, 1993. "Buckling of thin truncated conical shells (frusta) under quasi static and dynamic axial load". MSc Thesis, UMIST, UK

[12] Mamalis AG, Manolakos DE, Loannidis MB, Kostazos PK, 2005. "Numerical simulation of thin walled metallic circular frusta subjected to axial loading", Int. J. Crash-worthiness, 10, pp.505-13.

[13] Alghamdi AAA, Aljawi AAN, Abu-Mansour TMN, 2002. "Modes of axial collapse of unconstrained capped frusta". Int. J. Mech Sci, 44, pp.1145-61.

[14] Gupta N.K, Abbas H, 2000. "Axisymmetric axial crushing of thin frusta". Thin-Walled Struc, 36pp.169-79.

[15] Gupta N.K, Easwara Prasad GL, Gupta SK, 1997. "Plastic collapse of metallic conical frusta of large semi-apical angles". Int. J. Crash-Worthiness, 2, pp.349-66.